Proceedings of the ASME 2010 Pressure Vessels & Piping Division / K-PVP Conference
PVP2010
July 18-22, 2010, Bellevue, Washington, USA

PVP2010-25083

ACOUSTIC RESONANCE IN A RESERVOIR-PIPELINE-ORIFICE SYSTEM

Arris S. TIJSSELING
Department of Mathematics and Computer Science
Eindhoven University of Technology
P.O. Box 513, 5600 MB Eindhoven
The Netherlands
E-mail: a.s.tijsseling@tue.nl

Qingzhi HOU
Department of Mathematics and Computer Science
Eindhoven University of Technology
P.O. Box 513, 5600 MB Eindhoven
The Netherlands
E-mail: q.hou@tue.nl

Bjørnar SVINGEN
Rainpower FoU AS
S.P. Andersens veg 7
N-7465 Trondheim
Norway
E-mail: bjoernar.svingen@rainpower.no

Anton BERGANT
Litostroj Power d.o.o.
Litostrojska 50
1000 Ljubljana
Slovenia
E-mail: anton.bergant@litostrojpower.eu

ABSTRACT

The fundamentals of oscillating flow in a reservoir-pipe-orifice system are revisited in a theoretical study related to acoustic resonance experiments carried out in a large-scale pipeline. Four different types of system excitation are considered: forcing velocity, forcing pressure, linear oscillating resistance and nonlinear oscillating resistance. Analytical solutions are given for the periodic responses to the first three excitations. Analytical and numerical results for the large-scale pipeline are presented and some peculiarities are discussed.

Key words
Hydraulic transients; Acoustic resonance; Impedance; Orifice; Rotating valve; Analytical solution.

INTRODUCTION

Acoustic resonance in liquid-filled pipe systems is an undesirable phenomenon that cannot always be prevented. It causes noise, vibration, fatigue, instability, and it may lead to damage of hydraulic machinery and pipe supports. If possible, resonance should be anticipated in the design process and be part of the hydraulic transient analysis.

The prediction of resonance in liquid-filled pipelines is less straightforward than one might expect. First of all, the calculation of natural frequencies cannot always be based on simple formulas. Second, the excitation mechanism must be modelled correctly and care must be taken with excitation mechanisms that are influenced by the system response itself. Third, the influence and proper modelling of damping mechanisms is essential, in particular with regard to suppressing fluid transients and beat phenomena.

This study is a preliminary analysis of acoustic resonance tests carried out at Deltares, Delft, The Netherlands, within the framework of the European Hydralab III programme [1]. The (idealised) test system is a 50 m long pipeline of 200 mm diameter that is discharging water from a 25 m high reservoir through an 800 mm^2 orifice to the open atmosphere, as sketched in Fig.1. The outflow is partly interrupted by a rotating disc which generates flow disturbances at a fixed frequency in the range 3 Hz to 100 Hz. The system is simulated with four different models for the excitation.

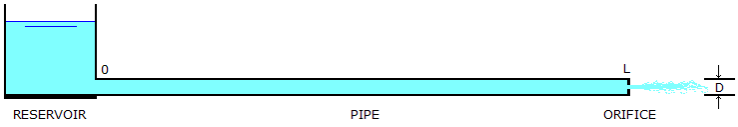

Figure 1. Sketch of reservoir-pipeline-orifice system; pipe length L = 50 m and inner diameter D = 0.2 m.

ABBREVIATIONS

DC = direct current
FSI = fluid-structure interaction
MOC = method of characteristics
TMM = transfer matrix method

Copyright © 2010 by ASME

WATERHAMMER EQUATIONS

Classical waterhammer theory [2-4] adequately describes the low-frequency vibration of elastic liquid columns in fully-filled pipes. The two equations, governing velocity, V, and pressure, P, are

$$\frac{\partial V}{\partial t} + \frac{1}{\rho}\frac{\partial P}{\partial x} = -\frac{\lambda_f}{2D} V|V| \ , \tag{1}$$

$$\frac{\partial V}{\partial x} + \frac{1}{K^*}\frac{\partial P}{\partial t} = 0 \ , \tag{2}$$

with

$$\frac{1}{K^*} := \frac{1}{K} + \frac{D}{Ee} \ . \tag{3}$$

Notation: D = inner pipe diameter, E = Young modulus of pipe material, e = wall thickness, K = bulk modulus of liquid, K^* = effective bulk modulus including wall elasticity, x = distance along pipe, t = time, λ_f = Darcy-Weisbach friction factor, and ρ = mass density of liquid. The friction term is ignored herein, i.e. $\lambda_f = 0$, to concentrate on the orifice as the sole cause of damping. Equations (1) and (2) can be combined to the standard wave equations

$$\frac{\partial^2 V}{\partial t^2} - c^2 \frac{\partial^2 V}{\partial x^2} = 0 \qquad \text{and} \qquad \frac{\partial^2 P}{\partial t^2} - c^2 \frac{\partial^2 P}{\partial x^2} = 0 \ , \tag{4a, 4b}$$

where the acoustic wave speed is

$$c := \sqrt{\frac{K^*}{\rho}} \ . \tag{5}$$

SINUSOIDAL EXCITATION

The pressure of the reservoir at $x = 0$ is taken constant, i.e.

$$P(0,t) = P_{\text{res}} \ . \tag{6}$$

Sinusoidal excitation at the downstream end (at $x = L$) is simply imposed by

$$V(L,t) = V(L,0) + \hat{V} \sin\left(2\pi \frac{t}{T}\right) \quad \text{or}$$

$$P(L,t) = P(L,0) + \hat{P} \sin\left(2\pi \frac{t}{T}\right) \ , \tag{7a, 7b}$$

where T is the period of oscillation, the circumflex (^) indicates the amplitude of oscillation, $V(L, 0) > \hat{V} > 0$ to prevent back-flow at $x = L$ and $P(L, t) = P_{\text{res}}$ to guarantee equilibrium for $\hat{V} = \hat{P} = 0$ or $T = \infty$.

In practice it may be difficult to realise one of the boundary conditions (7). Sinusoidal excitation has been achieved by two typical forcing devices: 1) the oscillating piston and 2) the oscillating valve. The frequency-controlled oscillating piston can excite the system directly [5-6] or indirectly (oscillating liquid column) [7-9]. Typical frequency-controlled valve designs among others include a servo-valve unit [10], a siren-type valve [11] and a unit with variable periphery disc [12]. In the Hydralab III project [1] a Svingen-type rotating disc [13] has been used, which is described by the orifice equation below. The Svingen-type valve has been proved to be a cost-effective device of simple and robust design (with negligible FSI effects on the pipe test section).

Nonlinear orifice equation

In steady turbulent pipe flow the pressure loss, ΔP_0, across an orifice is

$$\Delta P_0 = \xi_0 \tfrac{1}{2}\rho V_0 |V_0| \ , \quad \text{where} \quad \xi_0 := \left(\frac{A}{C_d\, A_{\text{or},0}}\right)^2 \ , \tag{8}$$

and V_0 is the steady flow velocity in the pipe, A is the cross-sectional area of the pipe, $A_{\text{or},0}$ is the steady outflow area of the orifice and C_d is the coefficient of discharge [2, Section 3-3], [14, Section 9-5]. In a quasi-steady manner, the same relation is assumed to hold for an orifice with an area that varies in time,

$$\Delta P = \xi(t) \tfrac{1}{2}\rho V |V| \ , \quad \text{where} \quad \xi(t) := \left(\frac{A}{C_d\, A_{\text{or}}(t)}\right)^2 \ , \tag{9}$$

and $\xi(0) = \xi_0$ when starting the area variation from steady state at $t = 0$. Dividing (9) by (8) and introducing the dimensionless valve closure coefficient $\tau(t) := \sqrt{\xi_0 / \xi(t)} = A_{\text{or}}(t) / A_{\text{or},0}$ gives the nonlinear boundary condition

$$\Delta P_0\, V|V| = \tau^2(t)\, V_0 |V_0|\, \Delta P \ , \quad V_0 \neq 0 \ , \tag{10}$$

where $\tau(t) = 1$ corresponds to the steady state. The specific function $\tau(t)$ used to generate oscillating flow is

$$\tau(t) := \frac{2-\alpha}{2} + \frac{\alpha}{2} \cos\left(2\pi \frac{t}{T}\right), \quad 0 \le \alpha \le 1 \ , \tag{11}$$

in which T is the period of the sinusoidal excitation and $\tau(0) = 1$, see Fig. 2. Equation (11) describes an orifice with

Copyright © 2010 by ASME

constant area $A_{or,0}$ that is partly covered by a varying area $A_{disc}(t)$ (rotating disc herein) according to the following relationships:

$$A_{or}(t) := A_{or}(0) - A_{disc}(t) \quad \text{with}$$

$$A_{disc}(t) := A_{disc,max}\left(\frac{1}{2} - \frac{1}{2}\cos\left(2\pi\frac{t}{T}\right)\right),\ 0 \le A_{disc,max} \le A_{or}(0) \tag{12a}$$

and

$$A_{or}(t) := A_{or}(0)\left(\frac{2-\alpha}{2} + \frac{\alpha}{2}\cos\left(2\pi\frac{t}{T}\right)\right) \quad \text{with}$$

$$\alpha := \frac{A_{disc,max}}{A_{or}(0)},\ 0 \le \alpha \le 1\ . \tag{12b}$$

Herein $A_{disc}(0) = 0$ and the initial orifice area at t = 0 is at largest, so that $A_{or}(0) = A_{or,0}$ and $1-\alpha \le \tau(t) \le 1$. This is in accordance with the experimental procedure, but of no importance for the final oscillatory steady state.

Linearised orifice equation

The orifice equation (10) is linearised around the initial steady state V_0, P_0 and τ_0 defined by relation (8) [2, Section 13-1]. This linearisation is needed for analysis in the frequency domain. Assuming flow discharging to the atmosphere, the pressure downstream of the orifice is taken zero, so that $\Delta P_0 = P_0$ and $\Delta P = P$. The small fluctuations v, p and τ' (*not* the derivative of τ) around the steady state are defined by

$$V := V_0 + v > 0,\quad v \ll V_0\ ;\quad P := P_0 + p > 0,\quad p \ll P_0\ ;$$
$$\tau := \tau_0 + \tau' > 0,\quad \tau' \ll \tau_0\ . \tag{13}$$

Substituting (13) into Eq. (10) and neglecting small quadratic terms gives

$$\frac{v}{V_0} - \frac{1}{2}\frac{p}{P_0} = \frac{\tau'}{\tau_0}\ . \tag{14}$$

The last term in Eq. (14) is zero for a fixed orifice and for Eq. (11) (with $\tau' = \tau - \tau_0$ and $\tau_0 = \tau(0) = 1$) it is

$$\tau'(t) = \frac{\alpha}{2}\left[\cos\left(2\pi\frac{t}{T}\right) - 1\right],\quad 0 \le \alpha \le 1\ . \tag{15}$$

The linearised excitation τ' has a non-zero average value of $-\alpha/2$, because V_0 is chosen to be the flow velocity for the orifice in its most open position.

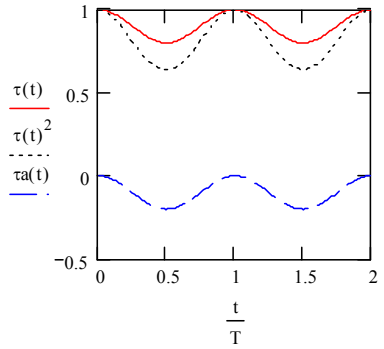

Figure 2. Functions $\tau(t)$, $\tau^2(t)$ and $\tau'(t)$ for $\alpha = 0.2$.

FUNDAMENTALS OF OSCILLATORY FLOW

The following basic relations are used: frequency $f = 1/T = c/\lambda$; angular frequency $\omega = 2\pi f = \kappa c$; wave number $\kappa = 2\pi/\lambda = \omega/c$; wave length $\lambda = 2\pi/\kappa = c\,T$.

Natural modes of oscillation

The flow in the reservoir-pipe-orifice system (Fig. 1) is excited sinusoidally at $x = L$. If the frequency of excitation is high enough, say f is of the order of c/L, the (elastic) liquid column will respond acoustically. In linear systems a steady oscillation builds up with a frequency equal to the constant frequency of excitation, something that is not necessarily the case when the nonlinear orifice equation (10) is applied. The amplitude of the oscillation strongly depends on the natural frequencies of the system, i.e. the frequencies of free vibration. For a system with a closed end (orifice area $A_{or,0}$ = 0) the fundamental natural frequency is $c/(4L)$ and the higher harmonics are the odd multiples of $c/(4L)$. For a system with an entirely open end (orifice area $A_{or,0} = A$) the fundamental frequency is $c/(2L)$ and the higher harmonics are the even multiples of $c/(4L)$. Figure 3 shows the first three modes of oscillation. For a system with an orifice (with area $0 < A_{or,0} < A$) the fundamental frequency is expected to be in between $c/(4L)$ and $c/(2L)$. The question is: could it – similar to a reservoir-pipe-(air-vessel) system [15] – become $c/(3L)$ (Fig. 4)? In that case the anti-node of the first mode is not necessarily at a boundary or at the midpoint.

Reservoir reflection point

Wave reflection does not exactly take place at x = 0, but somewhat into the reservoir. For short pipes this effect can be significant and instead of the nominal pipe length L an effective length L_{eff} should be used. Alster [16, Eq. 40] derived

$$\frac{L_{eff}}{L} = \sqrt{1 + 0.48\left(\frac{D}{L}\right)} \approx 1 + 0.24\frac{D}{L} \tag{16}$$

Copyright © 2010 by ASME

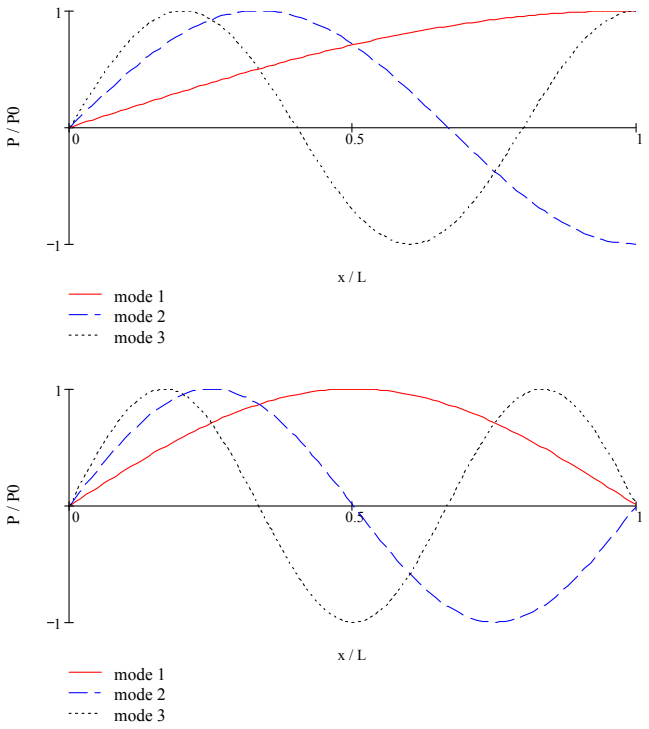

Figure 3. The first three basic modes of pressure oscillation relative to the steady state: closed end ($c/(4L)$, top) and open end ($c/(2L)$, bottom).

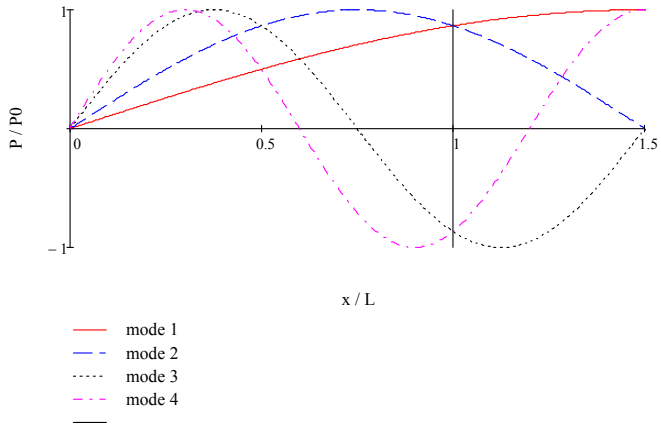

Figure 4. The first four $c/(3L)$ modes of pressure oscillation relative to the steady state with constant impedance $\left|\hat{P}/\hat{V}\right| = \rho c \tan(\pi/3)$ at $x = L$.

to account for added-mass effects in the (infinitely large) reservoir. The semi-empirical formula (16) is valid for circular ducts of inner diameter D. It differs from the classical $L_{\text{eff}}/L = 1 + 4/(3\pi)\,D/L \approx 1 + 0.42\,D/L$ given in standard textbooks on acoustics. In general L_{eff} will be dependent on the frequency of oscillation.

Orifice reflection criterion

For very small and very large apertures the orifice resembles a closed end and an open end, respectively. Based on *linear* theory (Eq. 14 with $\tau' = 0$), Wylie, Streeter and Suo [2, Section 12-5] found for the *free* vibration:

if $P_0 > \frac{1}{2}\rho c V_0$ the orifice behaves like a closed end (small pipe flow velocity means small orifice opening),

if $P_0 < \frac{1}{2}\rho c V_0$ the orifice behaves like a fully open end (large pipe flow velocity means large orifice opening),

if $P_0 = \frac{1}{2}\rho c V_0$ there is no reflection because the orifice impedance equals the system characteristic impedance.

(17)

There is a sudden jump in system behaviour as opposed to the gradual change in a reservoir-pipe-(air-vessel) system [15]. The system is either $c/(4L)$ or $c/(2L)$ and $c/(3L)$ will not occur. Criterion (17) has not (yet) been confirmed by time-domain solutions.

Resonance

In the studied pipe-flow system (Fig. 1), the orifice – with its rotating disc – is the exciter and the reservoir is the energy source. Resonance may develop when the orifice is in its most open position ($\tau(t) = \tau_{\max}$) when a low-pressure wave arrives and in its most closed position ($\tau(t) = \tau_{\min}$) when a high-pressure wave arrives. At resonance a standing wave – in fact an excited natural mode – dominates the system. The resonance criterion used herein is

$$\hat{V}_{\max} > 2\hat{V}_{\text{exc}} \quad \text{or} \quad \hat{P}_{\max} > 2\hat{P}_{\text{exc}}\,, \tag{18}$$

where $\hat{V}_{\text{exc}}$ or $\hat{P}_{\text{exc}}$ is the amplitude of the exciter and $\hat{V}_{\max}$ and $\hat{P}_{\max}$ are the calculated (or measured) maximal velocity and pressure responses. However, it is not always possible to clearly define $\hat{V}_{\text{exc}}$ or $\hat{P}_{\text{exc}}$.

Beat

Prior to the establishment of steady-oscillatory flow, a beat develops. The beat is the transient condition made up of the forcing function and the initial system response to the disturbance [2, p. 309]. Except for the start-up phase, beats may also develop when the forcing frequency is close to a natural

Copyright © 2010 by ASME

frequency of the system (e.g. in a spring-mass system). Because frequencies cannot coincide exactly, resonance often comes in the form of a beat. Two different forcing frequencies may also result in a beat. Beat is something unsteady (*not* steady-oscillatory), because the amplitude varies in time.

Wave-speed versus phase-velocity

Care must be taken in using the terms "wave speed" and "phase velocity". The wave speed is related to the front of a travelling disturbance and the phase velocity is related to a wave train (often of infinite length) [17]. The wave speed directly follows from a time-domain analysis and has values below the speed of sound in unconfined water (about 1480 m/s), whereas the phase velocity follows from a frequency-domain analysis and is a frequency-dependent complex number with absolute values possibly going up to infinity. The phase-velocity depends on the system's end conditions, whereas the wave speed does not. For dispersive waves it is difficult to identify the exact location of a wave front. Except for linear non-dispersive systems, wave speeds and phase velocities are *not* the same.

TIME-DOMAIN SOLUTION

The waterhammer equations (1) and (2), in combination with the boundary conditions (6), and (7) or (10), are solved exactly with the MOC-based method described in [18]. The quadratic equation (10) is solved simultaneously with one linear compatibility equation. This is done symbolically, but care should be taken of possible cancellation [19]. The initial condition is the undisturbed steady flow in the pipe. The reservoir pressure, P_{res}, and the resistance of the valve, ξ_0, determine the initial flow velocity according to relation (8).

In principle it is not handy to calculate steady-oscillatory solutions by time-marching from an undisturbed system, because it may take a (too) long time for transients to damp out. Special techniques have been developed to deal with this problem [20-24]. In addition, in finding the spectrum, each single frequency of excitation requires its own simulation. On the other hand, time-domain analysis is the only option if one wishes to include nonlinearities.

The symbolic steady-oscillatory solution of Eqs (4a), (6) with $P_{res} = 0$ and (7a) for velocity excitation with $V(x,0) = 0$, is [25]:

$$V_v(x,t) := \hat{V}\ \sin\left(2\pi\frac{t}{T}\right)\frac{\cos\left(2\pi\frac{x}{cT}\right)}{\cos\left(2\pi\frac{L}{cT}\right)} \quad \text{and}$$

$$P_v(x,t) := -\rho c\hat{V}\ \cos\left(2\pi\frac{t}{T}\right)\frac{\sin\left(2\pi\frac{x}{cT}\right)}{\cos\left(2\pi\frac{L}{cT}\right)}\ . \qquad (19a)$$

Resonance occurs when $2\pi\frac{L}{cT} = \frac{\pi}{2}\ (\mathrm{mod}\ \pi)$ which is equivalent to $f = \frac{c}{4L}\ (\mathrm{mod}\ \frac{c}{2L})$. The impedance at $x = L$ is $\left|\hat{P}_v/\hat{V}_v\right| = \rho c\tan\left(2\pi\frac{L}{cT}\right)$.

The symbolic steady-oscillatory solution of Eqs (4b), (6) with $P_{res} = 0$ and (7b) for pressure excitation with $P(x,0) = 0$, is:

$$P_p(x,t) := \hat{P}\ \sin\left(2\pi\frac{t}{T}\right)\frac{\sin\left(2\pi\frac{x}{cT}\right)}{\sin\left(2\pi\frac{L}{cT}\right)} \quad \text{and}$$

$$V_p(x,t) := \frac{\hat{P}}{\rho c}\cos\left(2\pi\frac{t}{T}\right)\frac{\cos\left(2\pi\frac{x}{cT}\right)}{\sin\left(2\pi\frac{L}{cT}\right)}\ . \qquad (19b)$$

Resonance occurs when $2\pi\frac{L}{cT} = 0\ (\mathrm{mod}\ \pi)$ which is equivalent to $f = \frac{c}{2L}\ (\mathrm{mod}\ \frac{c}{2L})$. The "resonance" at $f = 0$ represents rigid-column motion in one direction, which is oscillation with an infinitely large amplitude. The impedance at $x = L$ is $\left|\hat{P}_p/\hat{V}_p\right| = \rho c\tan\left(2\pi\frac{L}{cT}\right)$, too.

The analytical solutions (19a) and (19b) can be combined to satisfy any linear boundary condition at $x = L$. If one chooses

$$\hat{V} := \frac{\alpha}{2}\beta_0 V_0 \quad \text{and} \quad \hat{P} := \alpha\,\beta_0\,P_0 \quad \text{with}$$

$$\beta_0 := \frac{2\rho c V_0 P_0\tan\left(2\pi\frac{L}{cT}\right)}{\left[\rho c V_0\tan\left(2\pi\frac{L}{cT}\right)\right]^2 + 4{P_0}^2}\ , \qquad (19c)$$

in the Eqs (19a) and (19b), respectively, then the symbolic steady-oscillatory solution

$$V(x,t) := V_v(x,t) + V_p(x,t) - \hat{V} \quad \text{and}$$

Copyright © 2010 by ASME

$$P(x,t) := P_v(x,t) + P_p(x,t) \quad , \tag{19d}$$

satisfies the linearised orifice equation (14) with excitation (15). Equations (19) hold for zero initial conditions, but the steady states $V_0(x)$ and $P_0(x)$ may simply be added. Because τ' in Eq. (15) has a non-zero average, the velocity amplitude $\hat{V}$ has been subtracted in Eq. (19d). The ratio of pressure to velocity excitation at $x = L$ is $\left|\hat{P}/\hat{V}\right| = 2P_0/V_0$, from Eq. (19c). For constant impedance at $x = L$, that is $\tau' = 0$ in boundary condition (14), $|p/v| = 2P_0/V_0$ too. If, looking at criterion (17), $P_0 = \frac{1}{2}\rho c V_0$ the impedance equals the characteristic impedance ρc and there are no wave reflections at $x = L$. For $2P_0/V_0 = \rho c \tan(\pi/3)$ one might expect a system with $c/(3L)$ fundamental frequency (Fig. 4).

FREQUENCY-DOMAIN SOLUTION

Frequency-domain solutions can only be found for *linear* systems. The waterhammer equations (1) and (2), or (4), in combination with the boundary conditions (6), and (7) or (14), are solved exactly with the TMM-based approach described in [26]. For non-dispersive wave problems, TMM transfer-matrices and MOC transformation-matrices are directly related [26]. The transfer matrix relating sinusoidal velocity and pressure fluctuations at two locations (a distance Δx apart) is [2, Section 12-3]:

$$\begin{pmatrix} v_2 \\ p_2 \end{pmatrix} = \begin{pmatrix} \cos(\kappa\,\Delta x) & -\mathrm{i}\sin(\kappa\,\Delta x)/(\rho c) \\ -\mathrm{i}\sin(\kappa\,\Delta x)\,(\rho c) & \cos(\kappa\,\Delta x) \end{pmatrix} \begin{pmatrix} v_1 \\ p_1 \end{pmatrix} , \tag{20}$$

where the subscripts 1 and 2 indicate the positions x_1 and $x_2 = x_1 + \Delta x$ along the pipe. This matrix is to be combined with two boundary conditions to find v and p at both the upstream and downstream location. An elegant introduction to the usual notation with complex numbers is given by Goyder [27].

Frequency-domain analysis discloses natural modes and it directly leads to all steady-oscillatory solutions as a function of the forcing frequency. It is not handy for the calculation of (sharp) transient solutions, because the superposition of many natural modes of oscillation is needed to match the initial and boundary conditions.

TEST PROBLEM

The reservoir-pipe-orifice system is simulated with the following input data: pipe length L = 50 m, wave speed c = 1250 m/s, pipe flow area A = 31416 mm^2, orifice area $A_{or,0}$ = 800 mm^2, discharge coefficient C_d = 0.6, orifice cover fraction α = 0.2, reservoir pressure P_{res} = 2.5 bar, mass density ρ = 1000 kg/m^3 and friction factor λ_f = 0. These values correspond to an idealised laboratory system [1] with pipe inner diameter D = 200 mm, wall thickness e = 6 mm and the reservoir water-level $H_{res} \approx 25$ m above the elevation of the pipe's central axis. The small end effect included in L_{eff} = 50.05 m (Eq. 16) is neglected.

Orifice

The orifice is a horizontal slit of 100 mm width and 8 mm height. The atmospheric pressure downstream of the orifice has been set equal to zero, so that $P_0 = \Delta P_0$ and $P = \Delta P$ in Eqs (8-10) are gauge pressures. The resistance coefficient of the orifice is ξ_0 = 4284 from Eq. (8). With a frictionless pipe at constant initial pressure $P_0 = P_{res}$ = 250000 Pa, this gives a constant initial flow velocity V_0 = 0.342 m/s and a steady Reynolds number Re_0 = 68329. The neglected steady pressure loss due to skin friction along the pipe is $\lambda_f (L/D)(\rho V^2/2)$ = 292 Pa assuming that λ_f = 0.02. This is small compared to the steady pressure loss P_0 at the orifice.

Initially the orifice is fully open. At t = 0 the outflow is interrupted by a frequency-controlled rotating disc [12, 13] that has three 10 mm sinusoidal variations in its 263 mm radius as drawn in Fig. 5. The specific function $\tau(t)$ in Eq. (10) used to describe the orifice with rotating disc is

$$\tau(t) = 0.9 + 0.1\cos\left(2\pi\frac{t}{T}\right) , \quad \text{so that}$$
$$\tau'(t) = -0.1 + 0.1\cos\left(2\pi\frac{t}{T}\right) , \tag{21}$$

in which T is the period of the induced oscillation (see Fig. 2). The frequency range studied herein is from 1 Hz to 25 Hz. In its most closed position at $t/T = 1/2$ (mod 1) (Fig. 2) the orifice is a horizontal slit of 80 mm width and 8 mm height (Fig. 5) with resistance coefficient ξ_0 = 6693 from Eq. (8) and flow velocity V_0 = 0.273 m/s. If $\tau(t)$ = 0.9 (average τ-value) ξ_0 = 5288 and V_0 = 0.307 m/s. Thus, the velocity amplitude for very slow ($f \ll 1$ Hz) variations is $\hat{V}$ = 0.0342 m/s. Positive water displacements were needed for PIV measurements [1], so the induced flow is pulsating (not reversing direction).

Fundamental frequencies

The frequency range 1 Hz – 25 Hz covers the fundamental natural frequencies. If the forcing function is a velocity (Eq. 7a) the natural frequencies are (Eq. 19a): $c/(4L)$ = 6.25 Hz plus odd multiples of $c/(4L)$ (even harmonics are not excited). If the forcing function is a pressure (Eq. 7b) the natural frequencies are (Eq. 19b): $c/(2L)$ = 12.5 Hz plus even multiples of $c/(4L)$

Copyright © 2010 by ASME

(odd harmonics are not excited). If the forcing function is the quasi-steady orifice equation (10) with oscillating coefficient (11), it is a combination of velocity and pressure, and the fundamental frequency is not clear in advance. The decisive velocity according to Eq. (17) (*linear* theory, *free* vibration, Eq. 14 with $\tau' = 0$, small fluctuations) is $V_{0,\text{critical}} = 2P_0/(\rho c) =$ 0.4 m/s. Here V_0 is just below 0.4 m/s and the orifice is predicted to behave (as for the reflections) like a closed end (forcing velocity); for higher velocities it behaves like an open end (forcing pressure). The analytical solution (19cd) may shed further light on this matter.

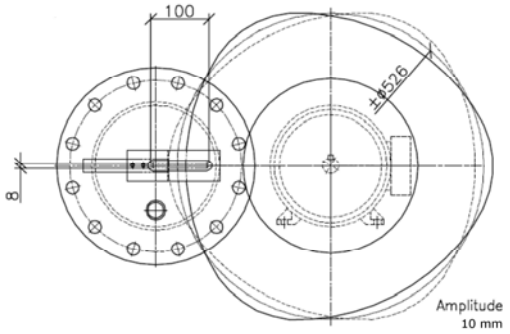

Figure 5. Front view of downstream pipe end with orifice and Svingen-type rotating disc.

SIMULATIONS

Velocity excitation

It is understandable that the periodically interrupted outflow is modelled by the velocity excitation (7a). First, the low-frequency behaviour is quasi-steady flow with a constant pressure $P_0 = 250000$ Pa and velocities varying in between $V_0 =$ 0.342 m/s and $V_0 = 0.273$ m/s, so that $\hat{V} = 0.0342$ m/s. Second, criterion (17) predicts closed-end ($V = 0$ and $\hat{V} = 0$) behaviour which corresponds to velocity-excitation with its imposed $c/(4L)$ fundamental frequency.

The analytical solution (19a) reveals that the maximum velocity amplitude $\hat{V}_{\max}$ occurs at $x = 0$, so that in absolute value it is (see Fig. 6)

$$\hat{V}_{\max}(f) = \frac{\hat{V}}{\left|\cos\left(2\pi \frac{L}{c} f\right)\right|} \quad . \tag{22}$$

The MOC time-domain solution [18] gives *exactly* the analytical solution (19a) only if the initial conditions are the same, that is: $V_0(x) = V_0$ and

$$P_0(x) = P_{\text{res}} - \rho c \hat{V} \sin\left(2\pi x/(cT)\right)\Big/\cos\left(2\pi L/(cT)\right).$$

The MOC solution differs from the analytical solution, if the time-marching does *not* start from the steady-oscillatory state. The difference is the transient generated – without the boundary excitation ($\hat{V} = 0$) – by the counter-balancing initial non-equilibrium $V_0(x) = V_0$ and

$$P_0(x) = P_{\text{res}} + \rho c \hat{V} \sin\left(2\pi x/(cT)\right)\Big/\cos\left(2\pi L/(cT)\right).$$

Figure 7 shows system responses for excitation frequencies of 1, 6 and 12 Hz. The dashed blue line is the steady-oscillatory solution (Eq. 19a) and the continuous red line is the MOC transient solution starting from the constant steady state $V_0(x) = V_0$ and $P_0(x) = P_{\text{res}}$. The velocities (at $x = 0$ and $x = L$) and pressures (at $x = L$) are displayed after subtraction of the steady state and the resulting oscillations are taken relative to the excitation amplitudes $\hat{V}$ and $\hat{P} = \rho c \hat{V}$. The steady-oscillatory velocities at $x = 0$ show an anti-node with maximal amplitude $\hat{V}_{\max}$, but the corresponding pressures at $x = L$ do not because the (first) pressure anti-node is at $x = cT/4 = \lambda/4$ which corresponds to $x = L$ only at resonance.

Equation (22) gives amplification factors $\hat{V}_{\max}/\hat{V}$ of 1.03, 15.9 and 1.01 for the excitation frequencies 1, 6 and 12 Hz, respectively. Resonance occurs at 6 Hz excitation, because this is close to the first natural frequency of 6.25 Hz [$c/(4L)$]. The transient response to 1 Hz excitation (Fig. 7a) includes waterhammer (free vibration) fluctuations with its characteristic frequency of 6.25 Hz. The effect is not so large [28], because the excitation time of 0.25 s (from zero to first peak) is larger than the wave-return time $2L/c = 0.08$ s, so that there is "no full Joukowsky" ($|P - P_0| < \hat{P} = \rho c \hat{V}$ at $x = L$), but about "half Joukowsky" (Fig. 7a). Full Joukowsky occurs for $f = 12$ Hz (Fig. 7c) where the waterhammer effect is maximal: $|P - P_0| / \hat{P}$ is about 1 here and $|V - V_0| / \hat{V}$ is about 2, because velocity waves double in magnitude upon reflection at the reservoir. This makes the waterhammer effect two times larger than the steady oscillation (Fig. 7c). The frequency-mismatch (12 Hz versus 6.25 Hz) leads to whimsical signals. Symmetry with respect to $t/T = 6$ (in transient V at $x = 0$) indicates a beat with a period of about $T/12$. The steady-oscillatory pressure at $x = L$ (dashed line) has low amplitude, because it is close to a node. Conversely, it is close to an anti-node when resonance occurs for $f = 6$ Hz (Fig. 7b). The steady-oscillatory flow has very large amplitude and the transient solution becomes a beat with its amplitude about twice so large and with a period of about $T/24$.

The problem here is – if one is interested in the steady-oscillatory situation only – that the initial transient does not die out at all, because one deals with a frictionless system. Optional line friction (lumped or distributed) will be small and gives rise to long simulation times, which is an annoyance especially in pipe networks [20-24]. The introduction of artificial damping that fades away in time would be an option. Frequency-domain solutions are fine and exact for this linearly modelled system.

Copyright © 2010 by ASME

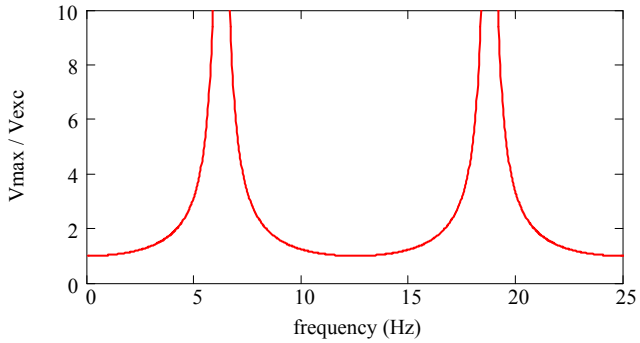

Fig. 6. Frequency response to velocity excitation ($V_{max} = \hat{V}_{max}$ and $V_{exc} = \hat{V}$).

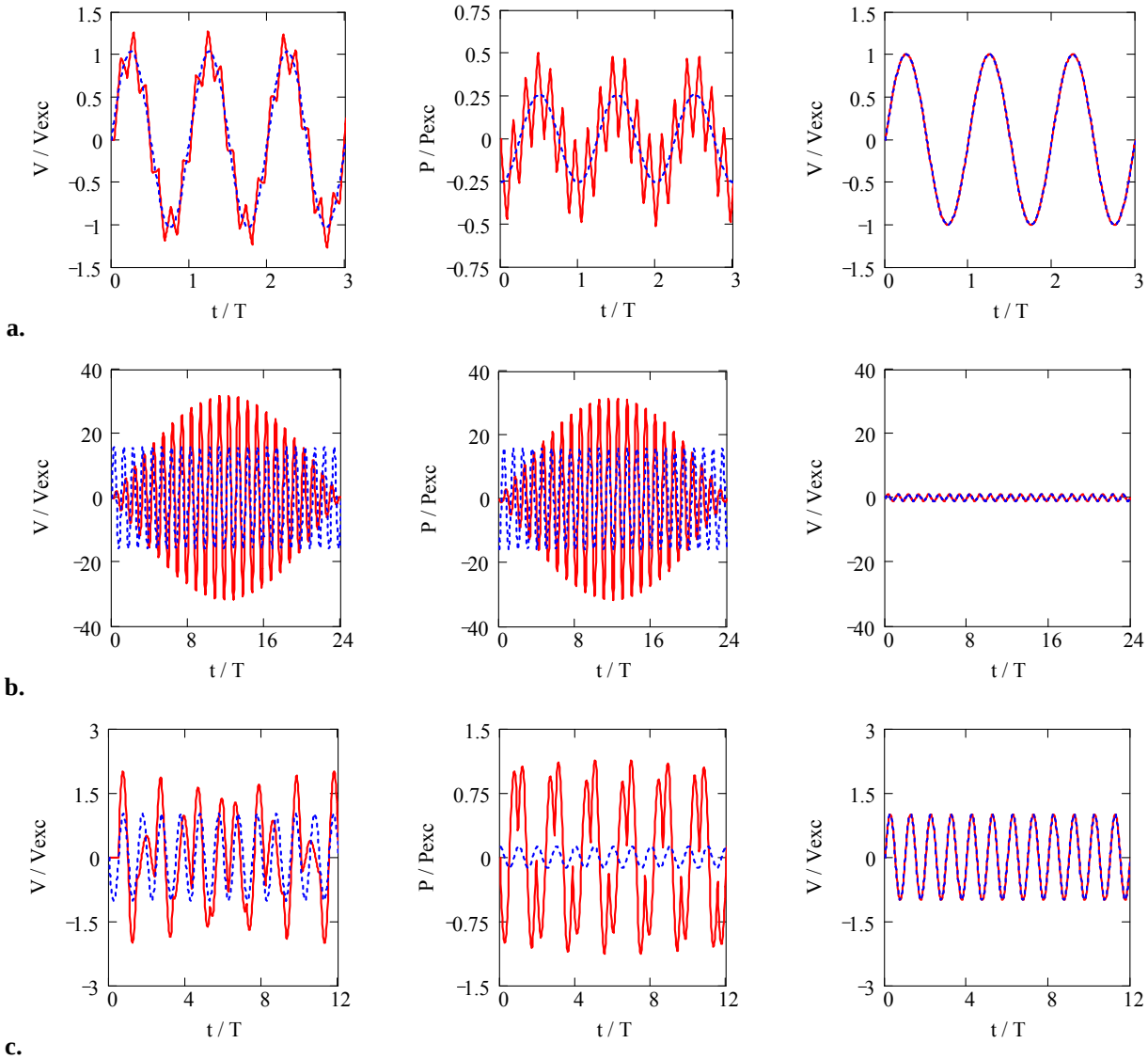

Figure 7. Velocity response (at $x = 0$), pressure response (at $x = L$) and velocity excitation (at $x = L$) at fixed frequency $f = 1/T$. Continuous line = transient solution; dashed line = steady-oscillatory solution (Eq. 19a); $V_{exc} = \hat{V}$ and $P_{exc} = \hat{P} = \rho c \hat{V}$;
a. $f = 1/T = 1$ Hz, **b.** $f = 1/T = 6$ Hz, **c.** $f = 1/T = 12$ Hz.

Copyright © 2010 by ASME

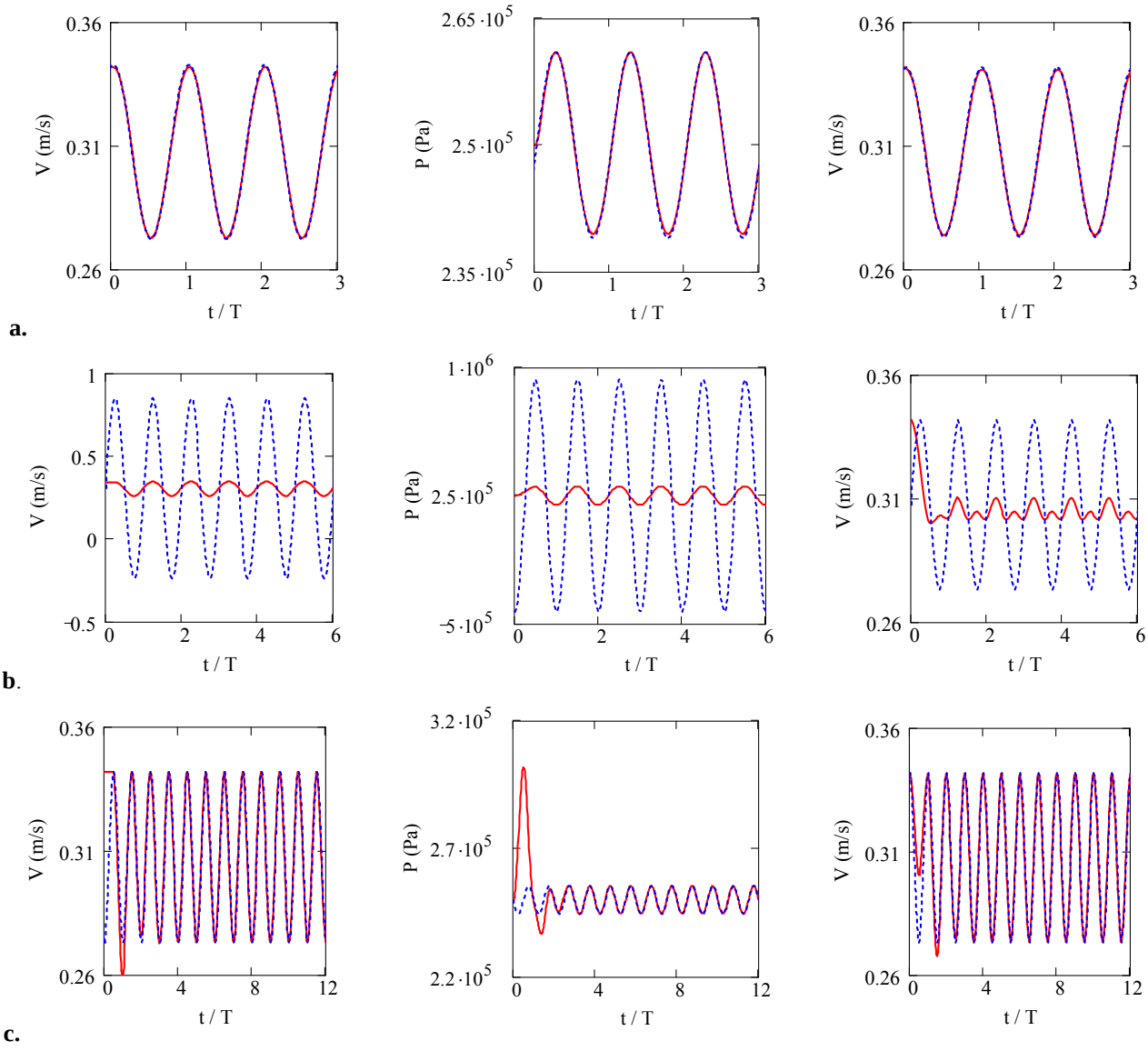

Figure 8. Velocity (at $x = 0$), pressure (at $x = L$) and velocity (at $x = L$) responses for nonlinear orifice excitation at fixed frequency $f = 1/T$. Continuous line = transient solution; dashed line = steady-oscillatory solution (forcing velocity, Eq. 19a); **a.** $f = 1/T = 1$ Hz, **b.** $f = 1/T = 6$ Hz, **c.** $f = 1/T = 12$ Hz.

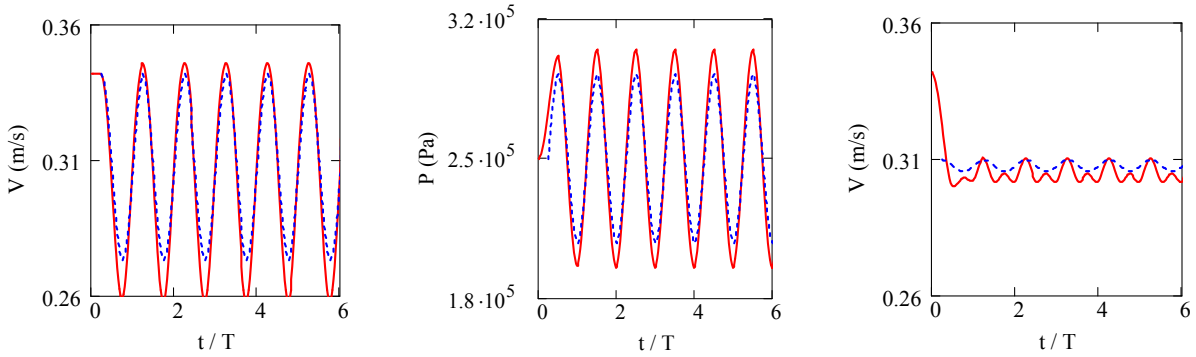

Figure 9. Velocity (at $x = 0$), pressure (at $x = L$) and velocity (at $x = L$) responses for nonlinear orifice excitation at fixed frequency $f = 1/T = 6$ Hz. Continuous line = transient solution; dashed line = steady-oscillatory solution (forcing pressure, Eq. 19b).

Copyright © 2010 by ASME

On the other hand, it is not wise to ignore the transient phase preceding the steady-oscillatory state, because the system pressures can be up to two times higher than the steady-oscillatory ones.

Nonlinear orifice excitation

This (Eqs 10 and 21) is the real excitation (except for any unsteady effects [29], which might be of significance near resonance). Figure 8 shows system responses for excitation frequencies of again 1, 6 and 12 Hz. The dashed blue line is the steady-oscillatory solution for forcing velocity (Eq. 19a) and the continuous red line is the MOC transient solution starting from the constant steady state $V_0(x) = V_0$ and $P_0(x) = P_{res}$. The velocities (at $x = 0$ and $x = L$) and pressures (at $x = L$) are *not* displayed after subtraction of the steady state, because in nonlinear systems the unsteady solution may depend on the initial steady state. Here the boundary condition (10) depends on the initial condition in a nonlinear way. Also, there are no clear excitation amplitudes $\hat{V}$ or $\hat{P}$ anymore to normalise velocities and pressures. The resulting oscillations are shown as they are, except that the steady-oscillatory solutions are shifted in time to make them in phase with the transient solutions.

One remarkable result is that for 1 Hz and 12 Hz excitation the transient dies out within two forcing cycles and the remaining steady-oscillatory solution is that of velocity excitation with $\hat{V} = 0.0342$ m/s. The initiated oscillation at the orifice is steady almost immediately at 1 Hz (Fig. 8a) and at 12 Hz (which is close to anti-resonance) the transient pressure peak is strongly damped (Fig. 8c). At 6 Hz it is a transient velocity drop that is strongly damped (Fig. 8b) and, compared to Fig. 7b, there is no strong resonance anymore. The velocity excitation is more or less replaced by a pressure excitation with $\hat{P} = \rho c \hat{V} = 42.7$ kPa as displayed in Fig. 9, where the steady-oscillatory solution (dashed line) is according to Eq. (19b).

Linear orifice excitation

Because the amplitude $\hat{V}$ of the forcing velocity is (exactly) 10% of the steady velocity V_0 herein, it is justified to use the linear approximation (14) with excitation (21). This linearisation is used in frequency-domain analyses. The only concern is that at resonance the amplitudes may become too large for the approximation to be valid, in particular if these occur at $x = L$. Indeed, the results obtained with either relationships (10) or (14) are very close to each other (not shown), except for a subtle difference in the velocities at the orifice as depicted in Figs 10 and 11. The steady-oscillatory state computed with MOC [18] matches the analytical solution (19cd) (not shown).

Discussion

The linear solution in Fig. 10a shows that at resonance the downstream velocity directly drops to a constant value of 0.307 m/s, which corresponds to steady flow with the orifice 90% open ($\tau = 0.9$ and $\tau' = -0.1$) as expected. The velocity and pressure oscillations are $\lambda/4$ modes (not shown). From Eq. (14) – with $v = 0$ – it is evident that the pressure fluctuation p directly follows the disc rotation represented by τ', such that $p = -2\tau'(t)P_0$.

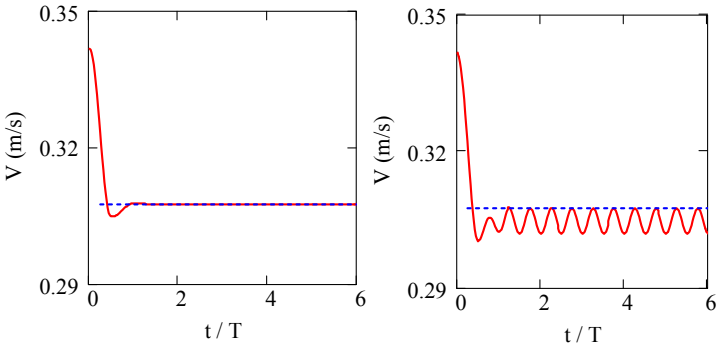

a. Linear solution. **b.** Nonlinear solution.

Figure 10. Velocity (at $x = L$) response for (**a**) linear and (**b**) nonlinear orifice excitation at resonance frequency $f = 1/T = 6.25$ Hz. Continuous line = transient solution; dashed line = steady-oscillatory solution (forcing pressure, Eq. 19b).

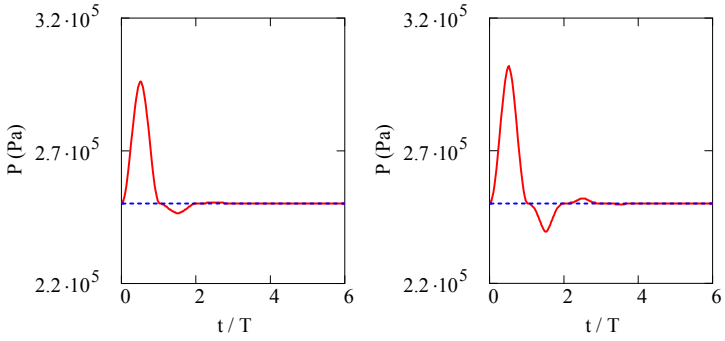

a. Linear solution. **b.** Nonlinear solution.

Figure 11. Pressure (at $x = L$) response for (**a**) linear and (**b**) nonlinear orifice excitation at anti-resonance frequency $f = 1/T = 12.5$ Hz. Continuous line = transient solution; dashed line = steady-oscillatory solution (forcing velocity, Eq. 19a).

The nonlinear solution in Fig. 10b shows that at resonance the downstream velocity is *not* constant, but oscillating at twice the resonance frequency around an average value below the expected 0.307 m/s (dashed blue line). The latter nonlinear effect is known as acoustic streaming [30]. Both frequency-

Copyright © 2010 by ASME

doubling and DC velocity shift result from Eqs (7a) and (10) in combination with the equality

$$\left[V_0 + \hat{V}\sin\left(2\pi\frac{t}{T}\right)\right]^2 = V_0^2 + \frac{1}{2}\hat{V}^2 + 2V_0\hat{V}\sin\left(2\pi\frac{t}{T}\right) - \frac{1}{2}\hat{V}^2\cos\left(4\pi\frac{t}{T}\right) \quad (23)$$

The frequency-doubling effect caused by an orifice has already been observed by Wood et al. [31], however without any further explanation. Average orifice aperture and average steady flow rate do not correspond anymore in the (quasi-steady) nonlinear orifice.

Away from resonance, with 1 Hz and 12 Hz excitation in Figs 8a and 8c, the transient dies out remarkably fast because the orifice introduces much damping and, compared to pure velocity and pressure excitation, a more realistic model of the interaction between system dynamics and orifice is used. For the 1 Hz case there is no transient at all, and for both the 1 Hz and 12 Hz cases the analytical solution (19a) gives excellent predictions of the periodic state. Near resonance the analytical solution (19b) is better. The change from velocity excitation away from resonance to pressure excitation near resonance can be fully explained from the analytical solution (19cd).

An apparent paradox in the linear model: at resonance (f = 6.25 Hz) the excitation is a forcing pressure and hence – at first sight – it is a $c/(2L)$ system (like Eq. 19b), but the constant outflow rate (Fig. 10a) makes it a $c/(4L)$ system (like Eq. 19a). However, at anti-resonance (f = 12.5 Hz) the outlet pressure is constant in the linear model (Fig. 11a), but this fact does *not* turn it into a $c/(2L)$ system; here the forcing velocity maintains it as a $c/(4L)$ system.

CONCLUSIONS

A frequency-controlled rotating valve that generates oscillating pipe flow in the acoustic range has been modelled in the time domain in four different ways: as a forcing velocity, as a forcing pressure, as a linear oscillating resistance and as a nonlinear oscillating resistance. Analytical steady-oscillatory solutions are presented for the first three cases. For the studied test case, away from resonance the forcing velocity is a simple and good model, except that fluid transients spoil the numerical solution. Near resonance the periodic behaviour transforms to that of a forcing pressure. The linear and nonlinear valve resistance models assure that fluid transients quickly damp out in the numerical simulations. The nonlinear model predicts near resonance a shift in the average outflow velocity and a doubling of its frequency of oscillation, where the linear model does not. The analytical solutions help in understanding and interpreting the results of the numerical simulations.

ACKNOWLEDGEMENTS

This study is part of the project *Unsteady friction in pipes and ducts* carried out at Deltares, Delft, The Netherlands, and was partially funded through EC-HYDRALAB III Contract 022441 (R113) by the European Union. The Chinese Ministry of Education is thanked for financially supporting the second author.

REFERENCES

[1] Vardy, A., Bergant, A., He, S., Ariyaratne, C., Koppel, T., Annus, I., Tijsseling, A., and Hou, Q., 2009, "Unsteady skin friction experimentation in a large diameter pipe", Proc. of the 3rd IAHR Int. Meeting of the Workgroup on Cavitation and Dynamic Problems in Hydraulic Machinery and Systems (Editor P. Rudolf), Brno, Czech Republic, October 2009, Paper P10, pp. 593-602.

[2] Wylie, E.B. and Streeter, V. L., 1993, *Fluid Transients in Systems*, Englewood Cliffs, New Jersey, USA: Prentice Hall.

[3] Bergant, A., Tijsseling, A.S., Vítkovský, J.P., Covas, D.I.C., Simpson, A.R., and Lambert, M.F., 2008, "Parameters affecting water-hammer wave attenuation, shape and timing – Part 1: Mathematical tools", IAHR Journal of Hydraulic Research, **46** (3), pp. 373-381.

[4] Bergant, A., Tijsseling, A.S., Vítkovský, J.P., Covas, D.I.C., Simpson, A.R., and Lambert, M.F., 2008, "Parameters affecting water-hammer wave attenuation, shape and timing – Part 2: Case studies", IAHR Journal of Hydraulic Research, **46** (3), pp. 382-391.

[5] Fanelli, M., Angelico, G., and Escobar, P., 1983, "Comprehensive experimental confirmation of transfer matrix theory for uniform pipelines under steady pulsating flow", BHRA, Proc. of the 4th Int. Conf. on Pressure Surges (Editor H.S. Stephens), Bath, UK, September 1983, pp. 379-391, ISBN 0-906085-87-X.

[6] Akhavan, R., Kamm, R.D., and Shapiro, A.H., 1991, "An investigation of transition to turbulence in bounded oscillatory Stokes flows, Part 1. Experiments", Journal of Fluid Mechanics, **225** (April), pp. 395-422.

[7] Baird, M.H.I., Round, G.F., and Cardenes, J.N. 1971, "Friction factors in pulsed turbulent flow", The Canadian Journal of Chemical Engineering, **49** (4), pp. 220-223.

[8] Jensen, B.L., Sumer, B.M., and Fredsøe, J., 1989, "Turbulent oscillatory boundary layers at high Reynolds numbers", Journal of Fluid Mechanics, **206** (September), pp. 265-297.

[9] Lodhal, C.R., Sumer, B.M., and Fredsøe, J., 1998, "Turbulent combined oscillatory flow and current in a pipe", Journal of Fluid Mechanics, **373** (October), pp. 313-348.

[10] D'Souza, A.F. and Oldenburger, R., 1964, "Dynamic response of fluid lines", ASME Journal of Basic Engineering, **86** (3), pp. 589-598.

Copyright © 2010 by ASME

[11] Ramaprian, B.R. and Tu, S.W., 1980, "An experimental study of oscillatory flow at transitional Reynolds numbers," Journal of Fluid Mechanics, **100** (3), pp. 513-544.
[12] Svingen, B., 1996, "Fluid structure interaction in piping systems", PhD Thesis, NTNU, Trondheim, Norway, ISBN 82-7119-981-1.
[13] Svingen, B., 1996, "Fluid structure interaction in slender pipes", BHR Group, Proc. of the 7th Int. Conf. on Pressure Surges and Fluid Transients in Pipelines and Open Channels (Editor A. Boldy), Harrogate, UK, April 1996, pp. 385-396; London, UK: Mechanical Engineering Publications, ISBN 0-85298-991-1.
[14] Vardy, A.E., 1990, *Fluid Principles*, Maidenhead, UK: McGraw-Hill.
[15] Tijsseling, A.S., Kruisbrink, A.C.H., and Pereira da Silva, A., 1999, "The reduction of pressure wave speeds by internal rectangular tubes", Proc. of the 3rd ASME & JSME Joint Fluids Engineering Conf., Symposium S-290 Water Hammer (Editor J.C.P. Liou), San Francisco, USA, July 1999, ASME - FED, Vol. 248, Paper FEDSM99-6903, Section 3.2, ISBN 0-7918-1978-7.
[16] Alster, M., 1972, "Improved calculation of resonant frequencies of Helmholtz resonators", Journal of Sound and Vibration, **24** (1), pp. 63-85.
[17] Leslie, D.J. and Tijsseling, A.S., 1999, "Wave speeds and phase velocities in liquid-filled pipes", Proc. of the 9th Int. Meeting of the IAHR Work Group on the Behaviour of Hydraulic Machinery under Steady Oscillatory Conditions (Editor L. Půlpitel), Brno, Czech Republic, September 1999, Paper E1, pp. 1-12.
[18] Tijsseling, A.S. and Bergant, A., 2007, "Meshless computation of water hammer", Proc. of the 2nd IAHR Int. Meeting of the Workgroup on Cavitation and Dynamic Problems in Hydraulic Machinery and Systems (Editors R. Susan-Resiga, S. Bernad and S. Muntean), Timişoara, Romania, October 2007, Scientific Bulletin of the "Politehnica" University of Timişoara, Transactions on Mechanics, Vol. 52(66), No. 6, pp. 65-76, ISSN 1224-6077.
[19] Bergant, A. and Simpson, A.R., 1991, "Quadratic-equation inaccuracy for water hammer", ASCE Journal of Hydraulic Engineering, **117** (11), pp. 1572-1574.
[20] Fox, J.A. and Keech, A.E., 1975, "Pipe network analysis – a novel steady state technique", Journal of the Institution of Water Engineers and Scientists, **29**, pp. 183-194.
[21] Vardy, A.E. and Chan L.I., 1983, "Rapidly attenuated water hammer and steel hammer", BHRA, Proc. of the 4th Int. Conf. on Pressure Surges (Editor H.S. Stephens), Bath, UK, September 1983, pp. 1-12, ISBN 0-906085-87-X.
[22] Shimada, M., 1988, "Time-marching approach for pipe steady flows", ASCE Journal of Hydraulic Engineering, **114** (11), pp. 1301-1320. [Discussed by J.A. Fox and A.E. Vardy in **116** (10), pp. 1295-1296.]
[23] Shimada, M., 1992, "Time-step control in TMA for steady flows in large pipelines", BHR Group, Proc. of the Int. Conf. on Pipeline Systems (Editors B. Coulbeck and E.P. Evans), Manchester, UK, March 1992, pp. 77-90, ISBN 0-7923-1668-1.
[24] Shimada, M., 1996, "Advances in theory and numerical techniques on time marching approach for steady flows in pipeline systems", BHR Group, Proc. of the 7th Int. Conf. on Pressure Surges and Fluid Transients in Pipelines and Open Channels (Editor A. Boldy), Harrogate, UK, April 1996, pp. 523-535; London, UK: Mechanical Engineering Publications, ISBN 0-85298-991-1.
[25] Barten, W., Manera, A., and Macian-Juan, R., 2008, "One- and two-dimensional standing pressure waves and one-dimensional travelling pulses using the US-NRC nuclear systems analysis code TRACE", Nuclear Engineering and Design, **238** (10), pp. 2568-2582.
[26] Zhang, L., Tijsseling, A.S., and Vardy A.E., 1999, "FSI analysis of liquid-filled pipes", Journal of Sound and Vibration, **224 (**1), pp. 69-99.
[27] Goyder, H., 2009, "On the modelling of noise generation in corrugated pipes", Proc. of the 2009 ASME Pressure Vessels and Piping Division Conf., Prague, Czech Republic, July 2009, Paper PVP2009-77321.
[28] Tijsseling, A.S. and Vardy, A.E., 2008, "Time scales and FSI in oscillatory liquid-filled pipe flow", BHR Group, Proc. of the 10th Int. Conf. on Pressure Surges (Editor S. Hunt), Edinburgh, United Kingdom, May 2008, pp. 553-568, ISBN 978-1-85598-095-2.
[29] Washio, S., Takahashi, S., Yu, Y., and Yamaguchi, S., 1996, "Study of unsteady orifice flow characteristics in hydraulic oil lines", ASME Journal of Fluids Engineering, **118** (4), pp. 743-748.
[30] Boluriaan, S. and Morris, P.J. , 2003, "Acoustic streaming: from Rayleigh to today", International Journal of Aeroacoustics, **2** (3-4), pp. 255-292.
[31] Wood, D.J., Dorsch, R.G., and Lightner, C., 1966, "Wave-plan analysis of unsteady flow in closed conduits", ASCE Journal of the Hydraulics Division, **92** (2), pp. 83-110.

Copyright © 2010 by ASME